

See discussions, stats, and author profiles for this publication at: <https://www.researchgate.net/publication/334051536>

Application of a resonance-based signal decomposition to the analysis of subtractive synthesizer filter resonances

Conference Paper · June 2019

CITATIONS

0

READS

112

3 authors, including:



Kemal Avci

Izmir Democracy University, Turkey, Izmir

29 PUBLICATIONS 170 CITATIONS

[SEE PROFILE](#)



Victor Lazzarini

National University of Ireland, Maynooth

85 PUBLICATIONS 352 CITATIONS

[SEE PROFILE](#)

Some of the authors of this publication are also working on these related projects:



Project

Ninth Workshop on Ubiquitous Music [View project](#)



Audio Engineering Society

Convention Paper 10177

Presented at the 146th Convention
2019 March 20–23, Dublin, Ireland

This Convention paper was selected based on a submitted abstract and 750-word precis that have been peer reviewed by at least two qualified anonymous reviewers. The complete manuscript was not peer reviewed. This convention paper has been reproduced from the author's advance manuscript without editing, corrections, or consideration by the Review Board. The AES takes no responsibility for the contents. This paper is available in the AES E-Library, <http://www.aes.org/e-lib>. All rights reserved. Reproduction of this paper, or any portion thereof, is not permitted without direct permission from the Journal of the Audio Engineering Society.

Application of a resonance-based signal decomposition to the analysis of subtractive synthesizer filter resonances

Joseph Timoney¹, Kemal Avci², and Victor Lazzarini¹

¹ Department of Computer Science, Maynooth University, Maynooth, Co.Kildare, Ireland

² Department of Electrical & Electronics Engineering, Izmir Democracy University, Izmir, Turkey

Correspondence should be addressed to Joseph Timoney (joseph.timoney@mu.ie)

ABSTRACT

This paper investigates the analysis of resonant filters as they appear in subtractive synthesizers. These filters and their properties are a key component in the synthesis chain. The work investigates the application of a new wavelet-like signal decomposition for examining the components that make up the filter output. It produces a pair of ‘low’ and ‘high’ components. The results will examine these components spectrally with the intention that they might lead to new insights into synthesis and modeling.

1 Introduction

Although over 50 years old Subtractive synthesis is still a very popular approach for creating electronic sounds [1]. The basic idea behind subtractive synthesis is to have at least one oscillator, but more commonly two, generating non-sinusoidal timbrally-rich waveforms. Typically, these are sawtooths, pulse waves and triangles. Their octave and tuning is controllable. Once the waves are mixed together, their timbre is modified using a filter, this is the subtractive element. The filter has a number of user-adjustable parameters. Finally, the volume of the waveform is shaped over time using an envelope generator in the amplifier section before output. A common configuration for this is ADSR (Attack-Decay-Sustain-Release). The relative ease by which the principles of this synthesis technique can be understood, the wide variety of the sounds that can be generated, and the sonic beauty that can be

created have all contributed to its lasting popularity among musicians.

It is thus clear that a key part of the subtractive synthesizer system is the filter section. This is really felt by many musicians to impart the strongest sense of character between the many varieties of instruments that exist [2]. This is true in both the worlds of analog and digital synthesis. Even a brief glance at the many web forums about synthesizers will find many opinions on the sound characteristics and applicability of various filter configurations and their implementations.

The filter section of a subtractive synthesizer will always have a lowpass filter and sometimes a high pass filter or multimode version is available too. The filter is most often of a 12dB/octave or 24 dB/octave variety, though those with other slopes have appeared in the marketplace. The controls associated with the filter are the Cutoff and Resonance [3], where Cutoff determines the point at which the filtering takes effect while the Resonance defines an added emphasis to the filter

response in the vicinity of the cutoff frequency that is achieved using feedback [3] [4] and [5]. This resonance is very important when sweeping the filter cutoff as it really makes the sweeping movement much more perceptible. This sweeping of the filter cutoff can be done manually but typically is it done using another ADSR envelope, triggered at the same time at the amplifier envelope, but with its own set of controls. Higher settings for the resonance gives greater prominence to the sweep effect. Another associated phenomenon with Resonance is termed as filter self-oscillation. In some filters you can increase the resonance control up to a point that the filter response becomes very narrow, so much so that the filter output is perceived to be almost like a sine wave, having a rough whistling type of sound [2]. This sound can be played using the keyboard in a semi-tuneful manner with the normal oscillators turned off. The resonant sound of the filter is particularly important in certain genres of music, such as Acid House, that is closely associated with the TB-303 bassline synthesizer [6].

To date there has been no specific analysis of subtractive synthesizer filter resonances, all work has been focused on analyzing the behavior complete filter. However, knowledge about the resonance itself may offer unforeseen insights to these devices. It should be noted that the resonant filter output is rarely pure: the sound of the MiniMoog is partly because its filter was overdriven according to the designer [7] and similarly for the Korg MS-20. Such insights may be helpful for computationally efficient non-circuit-based emulations of classic subtractive synthesis filters as well as for devising new sound synthesis algorithms and instruments.

A new tool has emerged in the form of a new nonlinear signal transform that could provide an alternative perspective from which to investigate the filter resonance phenomenon. This signal analysis method is based on the property of signal resonance, rather than on frequency or scale. It is proposed to express a signal as the sum of a ‘high-resonance’ and a ‘low-resonance’ component [8] — a high-resonance component being a signal consisting of multiple simultaneous sustained oscillations; a low-resonance component being a signal consisting of non-oscillatory transients of unspecified shape and

duration. This offers a novel perspective on how the resonant waveforms recorded from synthesizers could be decomposed, separating out sustained and transitory signal phenomena.

The next section will first present some example resonant waveforms recorded from a two analog and one digital filter from Moog, Oberheim, and Access Virus respectively. The waveforms are generated specifically to have a transient at the beginning followed by a sustained oscillation. The section following this will give more detail on the Resonance-based signal decomposition and its implementation using wavelets, Results will be given in the next section followed by a closing section with conclusions and future work.

2 Example of Resonant waveforms

To investigate the impact of the decomposition it was decided to create four example waveforms that had a transient and sustained oscillation. Simplicity was desired. Three synthesizers were chosen: A Moog Voyager, A new edition Oberheim SEM, and an Access Virus KB. In all cases the synthesizer settings were as given in the table below

Parameter	Setting
Oscillator Waveform	Sawtooth
Oscillator Pitch	C4
Oscillator LFO	Off
Oscillator Mix	Oscillator 1 only
Filter Cutoff	30%
Filter Envelope Depth	Maximum
Resonance	Maximum
Filter A-D-S-R	20% -min-max-min
Amplifier A-D-S-R	min -min-max-min

Table 1. Synthesizer Parameter settings.

In the case of the Filter ASDSR the attack is set such that a short transient is generated at the beginning of the waveform by the sweeping filter. The recordings were using Audacity and with a Tascam US-MKII sound card for the input. Figure 1, 3 and 5 show the resulting waveforms and Figures 2, 4, 6 the spectrograms of the waveforms. The top panel in Figures 1, 3 and 5 shows the recorded waveform

from the synthesizer. In the bottom panel these have been divided in to the transient in the left plot and a zoomed region of the sustained portion in the right plot.

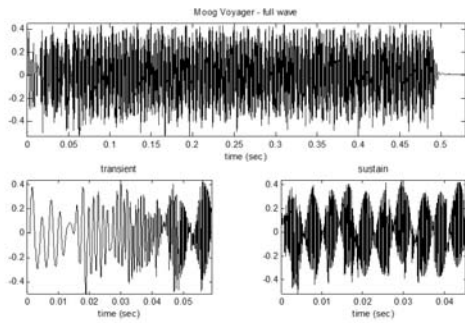


Figure 1. Recorded waveform (top) from a Moog Voyager analog synthesizer. On the bottom the transient on the left and the sustained wave on the right.

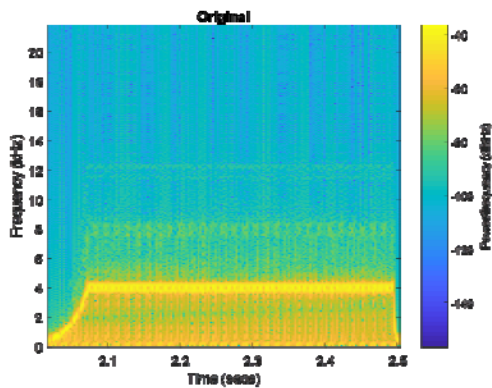


Figure 2. Spectrogram of Moog Voyager waveform.

The waveforms in the top panel of Figures 1, 3, and 5 for each synthesizer are quite different in appearance, even though for a single sawtooth oscillator, which reflects the unique character of each instrument. From all the plots in the bottom left panel the transient is approximately less than 100msec in duration in each recording. The cause of the transient is when the filter first engages with the sawtooth waveform it sweeps rapidly from the cutoff

frequency to the maximum frequency determined by the envelope amount. This is manifested in the waveform having a chirp-like appearance as different frequency components in the waveform become emphasized during the sweep.

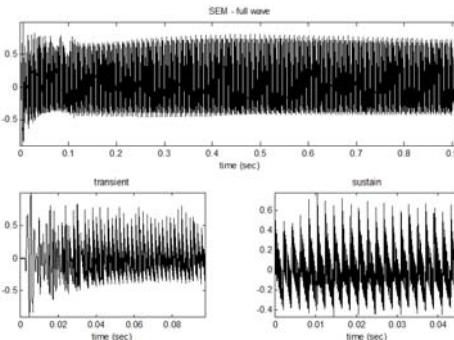


Figure 3. Recorded waveform (top) from an SEM analog synthesizer. On the bottom the transient on the left and the sustained wave on the right.

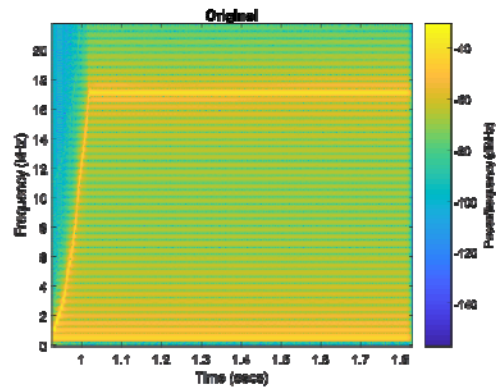


Figure 4. Spectrogram of SEM waveform

The spectrograms for the waveforms are given in Figures 2, 4, and 6. It is clear from the spectrograms the trajectory of the resonance in the frequency domain. Note that comparing Figure 2 and Figure 4, the Moog and SEM spectrograms, the Moog has a 24 dB/oct filter while the SEM has a 12 dB/oct and has more higher harmonics in the SEM spectrogram reflecting the weaker attenuation of its filter.

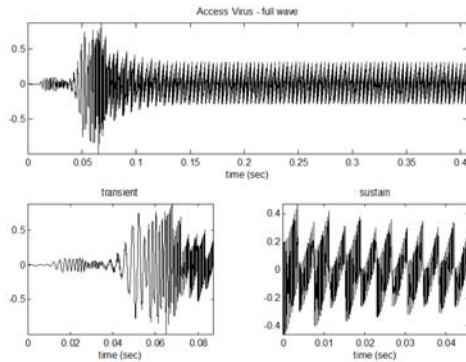


Figure 5. Recorded waveform (top) from an Access Virus digital synthesizer. On the bottom the transient on the left and the sustained wave on the right.

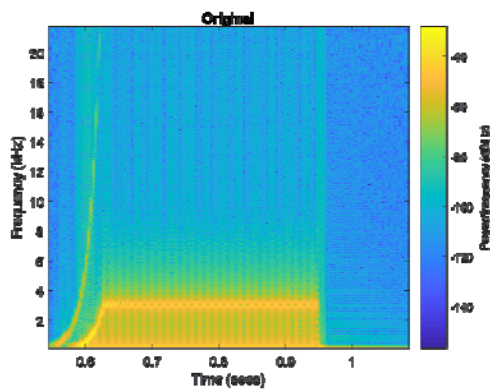


Figure 6. Spectrogram of Access Virus waveform.

In all waveform examples the sustained portion has quite a different shape and this is matched in the perceived sound.

The next section will describe the signal decomposition method.

3 Signal decomposition

The motivation for this decomposition came from the observation that many complex signals arising from physiological and physical processes are not only non-stationary but also exhibit a mixture of oscillatory and non-oscillatory transient behaviors. The method expresses a signal as the sum of a 'high-

resonance' and a 'low-resonance' component. This low-resonance and high-resonance components of a signal cannot be simply extracted from the signal by frequency-based filtering. This renders the resonance-based signal decomposition to be a difficult problem that requires a nonlinear approach, computed numerically by an iterative optimization algorithm.

The method presented in [8] for computing the high- and low-resonance components of a signal is based on the efficient representation of these two signal components using two suitably designed bases. The efficient representation of the high-resonance signal component requires a basis ideally comprised entirely of high-resonance functions. These should be high Q-factor (or quality-factor) functions where the quality-factor measures the ratio of the center frequency to the bandwidth. Such a basis can be obtained from a single high Q-factor pulse by translating and time-scaling it. Similarly, for the efficient representation of the low-resonance signal component it needs a basis comprised entirely of low-resonance (low Q-factor) functions; which can likewise be obtained from a single low Q-factor pulse through translation and time-scaling. The actual algorithm uses a rational-dilation wavelet transform (RADWT) for the sparse representation of each resonance component. The RADWT is a self-inverting fully-discrete transform. A Matlab toolbox is available at [1] [8].

4 Application to resonance waveforms

The decomposition technique was applied to the waveforms and the outputs were recorded. In the experiments cases two factors for decomposing the low and high resonance components respectively were used: $Q_1=1$ and $Q_2=2$; $Q_1=1$ and $Q_2=10$. The spectrograms of the outputs for the Moog waveform are shown in Figures 7-10.

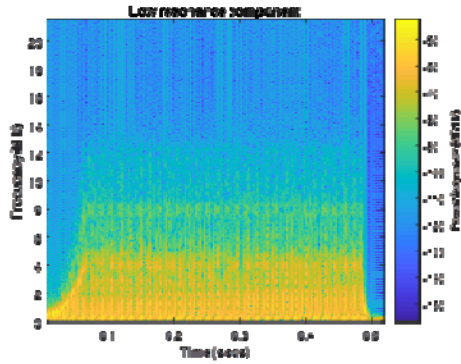


Figure 7. Spectrogram of Moog Voyager Low Resonance Component $Q_1=1$ and $Q_2=2$.

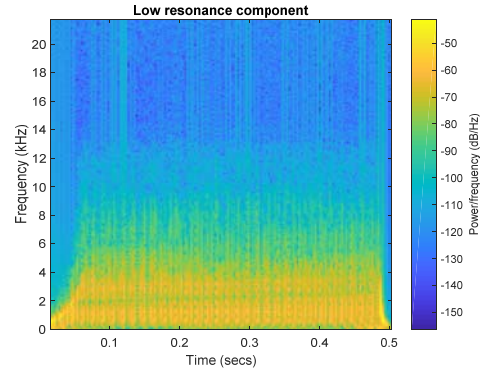


Figure 9. Spectrogram of Moog Voyager Low Resonance Component $Q_1=1$ and $Q_2=10$.

First of all from the figures it is clear that the decomposition is not strictly separating the waveform into a transient and sustained component. It appears to be isolating the components in the vicinity of the enhancing resonance as in Figures 8 and 10 and the remainder as shown in Figures 7 and 9.

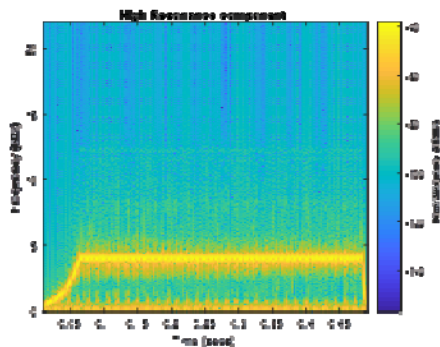


Figure 8. Spectrogram of Moog Voyager High Resonance Component $Q_1=1$ and $Q_2=2$.

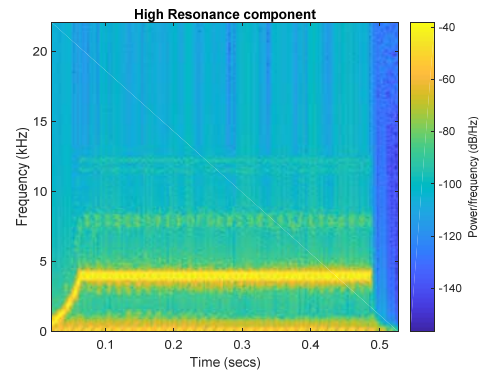


Figure 10. Spectrogram of Moog Voyager High Resonance Component $Q_1=1$ and $Q_2=10$.

The same behavior can be observed for the SEM waveform.

Comparing Figures 7 and 9 and Figures 8 and 10 with each other it can be seen that the second decomposition gives slightly stronger separation between the resonance components and the other components as there seems to be less energy either side of the resonance in Figure 10 compared to Figure 8.

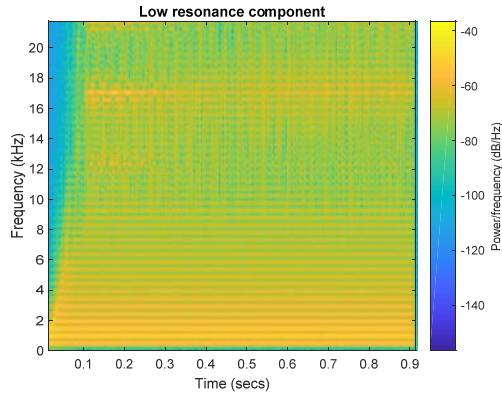


Figure 11. Spectrogram of SEM Low Resonance Component $Q_1=1$ and $Q_2=2$.

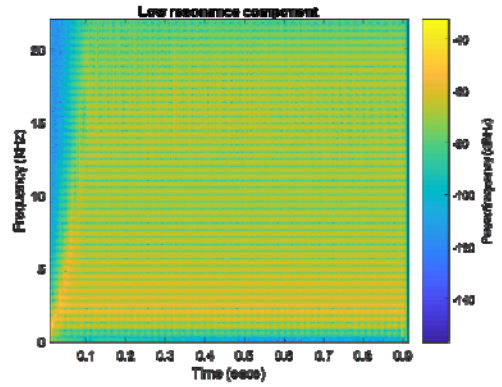


Figure 13. Spectrogram of SEM Low Resonance Component $Q_1=1$ and $Q_2=10$.

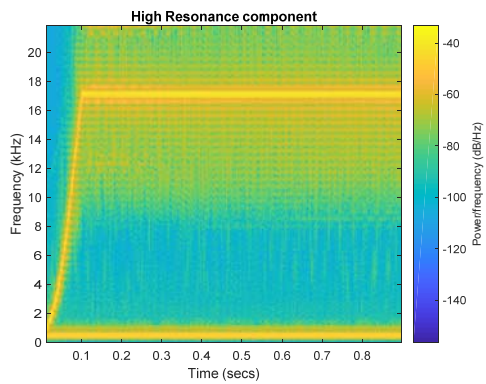


Figure 12. Spectrogram of SEM High Resonance Component $Q_1=1$ and $Q_2=2$

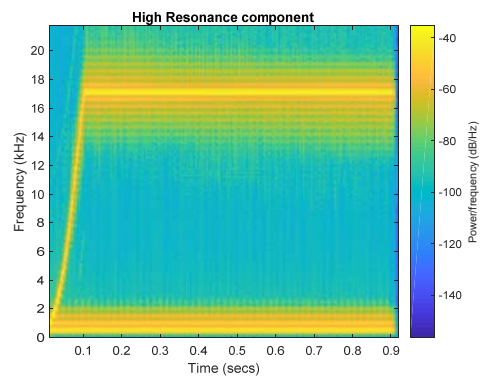


Figure 14 Spectrogram of SEM High Resonance Component $Q_1=1$ and $Q_2=10$.

Figure 11-14 show the spectrograms of the decomposition signals for the SEM waveform. Comparing Figure 11 and 13 and Figures 12 and 14 it can be observed that again there is a slightly clearer separation between the resonance signals and the remainder for the case where $Q_1=1$ and $Q_2=10$.

Lastly for the Access Virus Figures 15-18 show the spectrograms of the outputs. The observation is again replicated with the between separation between resonance and remainder in Figures 17 and 18 for $Q_1=1$ and $Q_2=10$.

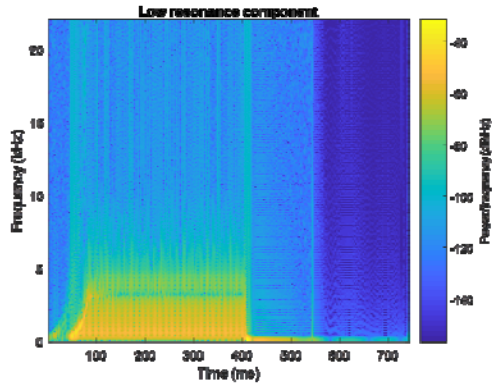


Figure 15. Spectrogram of Access Virus Low Resonance Component $Q_1=1$ and $Q_2=2$.

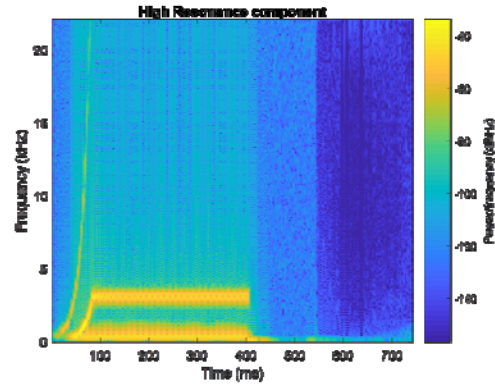


Figure 18. Spectrogram of Access Virus High Resonance Component $Q_1=1$ and $Q_2=10$.

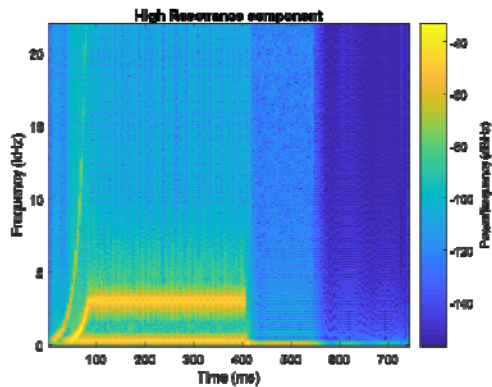


Figure 16. Spectrogram of Access Virus High Resonance Component $Q_1=1$ and $Q_2=2$.

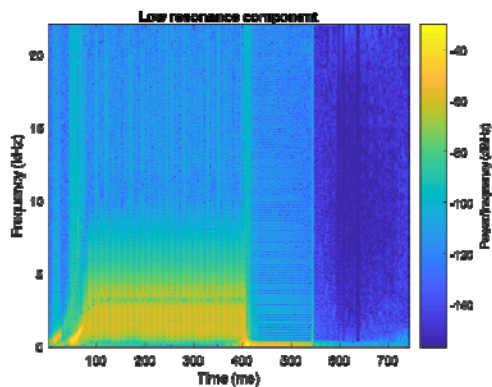


Figure 17. Spectrogram of Access Virus Low Resonance Component $Q_1=1$ and $Q_2=10$.

5 Conclusion and future work

From the results it can be seen from the spectrograms that the Signal resonance decomposition can be used to separate the resonant synthesizer signal into two components. The original paper presents the method as one that separates a signal into a High resonance component that is a sustained oscillation and a Low resonance component should be a transitory non-oscillatory component. In application of the method it was discovered from analyzing the spectrograms that one of the output components follows the high filter resonance and the other is the signal remaining. Using parameter values of $Q_1=1$ and $Q_2=10$ gives a better separation between the two.

Future work will develop more experiments to analyse the properties of the decomposition. Complicated filter resonance signals will be created for a variety of filter ADSR values. A deeper investigation will be made to understand more thoroughly the impact of the Q-factors. Lastly, a comparison will be made with the related Empirical Mode Decomposition [10] which converts a multicomponent signal into several narrow-band AM-FM components (intrinsic mode functions).

References

- [1] M. Russ, *Sound Synthesis and Sampling*, Oxford, UK: Focal Press; 3 Edition, 2008.
- [2] S. Riesterer, "Synthesis Essentials: Know Your Filters," AskAudio, [Online]. Available: <https://ask.audio/articles/synthesis-essentials-know-your-filters>. [Accessed Nov. 2018].
- [3] T. Stinchcombe, "Analysis of the Moog Transistor Ladder and Derivative Filters," http://www.timstinchcombe.co.uk/index.php?pge=synth#moog_paper, 2008.
- [4] T. Stilson and J. Smith, "Analyzing the Moog VCF with Considerations for Digital Implementation," in *Proc. International Computer Music Conference*, Hong Kong, 1996.
- [5] E. Paschou, F. Esqueda, V. Välimäki and J. Mourjopoulos, "Modeling and Measuring a Moog Voltage-Controlled Filter," in *Proc. Asia-Pacific Signal and Information Processing Association Annual Summit and Conference (APSIPA ASC)*, Kuala Lumpur, 2017.
- [6] "Roland TB-303 acid house flashback," Roland Inc., [Online]. Available: <http://www.roland.co.uk/blog/tb-303-acid-house-flashback/>. [Accessed Nov 2018].
- [7] M. M. Inc., "A brief history of the Minimoog Part 1: interview with Bill Hemsath," YouTube, [Online]. Available: https://www.youtube.com/watch?v=sLx_x5Fuzp4. [Accessed Nov. 2018].
- [8] I. Selesnick, "Resonance-based signal decomposition: A new sparsity-enabled signal analysis method," *Signal Processing*, vol. 91, no. 12, pp. 2793-2809, 2011.
- [9] I. Selesnick, "Rational-Dilation Wavelet Transforms (RADWT)," Jan. 2019. [Online]. Available: <http://eeweb.poly.edu/iselesni/rational/index.html>.
- [10] G. Rilling, P. Flandrin and P. Gonçalves, "On empirical mode decomposition and its algorithms," in *IEEE-EURASIP workshop on nonlinear signal and image processing, NSIP-03*, Grado, Italy, 2003.